iranpaper Downloaded from https://iranpaper.ir
https://www.tarjomano.com ترجمه تخصصی این مقاله مورد تایید ایران پیپر

Journal of the Taiwan Institute of Chemical Engineers 180 (2026) 106461

Contents lists available at ScienceDirect

Journal of the Taiwan Institute of Chemical Engineers

journal homepage: www.journals.elsevier.com/journal-of-the-taiwan-institute-of-chemical-engineers

Dynamic Simulation and Optimization of an Innovative Cogeneration System Using TRNSYS, EES, and Response Surface Methodology as a Machine learning method

Ali Dezhdar [a,1], Ehsanolah Assareh [a,b,1,*], Jagadeesh Kumar Alagarasan [c,1,*], Mehdi Hosseinzadeh [d,e], Saurabh Agarwal [f,1], Saleh Mobayen [g,*], Neha Agarwal [h,*]

[a] Strategic Research Institute (SRI), Asia Pacific University of Technology and Innovation (APU), Technology Park Malaysia, Kuala Lumpur, Malaysia
[b] Renewable Energy and Energy Efficiency Group, Department of Infrastructure Engineering, Faculty of Engineering and IT, The University of Melbourne, Australia
[c] Department of Chemistry, Faculty of Science, Technology and Architecture (FoST&A), Manipal University Jaipur, Jaipur, 303007, Rajasthan, India
[d] School of Engineering & Technology, Duy Tan University, Da Nang, Vietnam
[e] Department of AI, School of Computer Science and Engineering, Galgotias University, Greater Noida, India
[f] School of Computer Science and Engineering, Yeungnam University, Gyeongsan, 38541, South Korea
[g] Graduate School of Intelligent Data Science, National Yunlin University of Science and Technology, Douliu, Yunlin, 640301, Taiwan
[h] School of Chemical Engineering, Yeungnam University, Gyeongsan, 38541, South Korea

ARTICLE INFO

Keywords:
Solar-powered cogeneration
Organic Rankine cycle
TRNSYS–EES integration
Response Surface Methodology
Multi-objective optimization
Reverse osmosis desalination

ABSTRACT

The rapid growth in global energy demand, coupled with the urgent need to reduce greenhouse gas emissions, necessitates the development of sustainable, multi-output energy systems. This study presents the design, simulation, and optimization of an innovative solar-powered cogeneration system capable of simultaneously meeting the annual electricity, heating, cooling, and freshwater demands of a 100-unit residential complex in Tehran, Iran. The proposed configuration integrates a solar dish concentrator, organic Rankine cycle (ORC), heat pump, reverse osmosis desalination, hot and cold water storage tanks, and an auxiliary boiler. Dynamic simulations were conducted using TRNSYS, with thermodynamic modeling of the ORC performed in Engineering Equation Solver (EES). A multi-objective optimization framework, based on Response Surface Methodology (RSM) in Design Expert, was applied to minimize life cycle cost (LCC), boiler fuel consumption, and electricity usage, while maximizing thermal comfort (predicted mean vote, PMV).The optimal design—comprising a 101.25 m^2 solar dish, 20.27 kW cooling capacity, 36.29 kW heating capacity, and benzene as the ORC working fluid—achieves an LCC of $134,130, annual boiler fuel consumption of 6,918.0 m^3, and electricity consumption of 6,437.4 kWh, while producing freshwater with a total dissolved solids (TDS) level below 500 mg/L in compliance with WHO drinking water standards. Compared with a conventional PV + grid + boiler system, the proposed design reduces the LCC by 18.4% and annual CO_2 emissions by over 13 tonnes. Although benzene emerged as optimal in the numerical optimization, alternative low-global-warming-potential fluids such as R1233zd(E) are discussed as safer, environmentally favorable options with minimal efficiency trade-offs. In particular, R1233zd (E) and toluene are highlighted as practical alternatives, balancing acceptable efficiency with improved safety and environmental compliance. Beyond the Tehran case study, a dimensionless scaling approach is proposed for adapting the system to other climatic zones, enabling re-optimization of key parameters such as solar dish area and heat pump capacities based on local meteorological and demand profiles. The results demonstrate that the integrated TRNSYS–EES–RSM framework can deliver cost-effective, environmentally sustainable, and technically robust cogeneration solutions for residential applications in sun-rich regions.

* Corresponding authors.
E-mail addresses: Ehsanolah.assareh@unimelb.edu.au (E. Assareh), jaga.jagadeesh1987@gmail.com (J.K. Alagarasan), mobayens@yuntech.edu.tw (S. Mobayen), cheneha9@gmail.com (N. Agarwal).
[1] These authors contributed equally to this article as the first author.

https://doi.org/10.1016/j.jtice.2025.106461
Received 22 April 2025; Received in revised form 20 September 2025; Accepted 2 October 2025
Available online 15 October 2025
1876-1070/© 2025 Taiwan Institute of Chemical Engineers. Published by Elsevier B.V. All rights are reserved, including those for text and data mining, AI training, and similar technologies.

iranpaper Downloaded from https://iranpaper.ir
https://www.tarjomano.com ترجمه تخصصی این مقاله مورد تایید ایران پیپر

Nomenclature

Abbreviation Definition

CPC	Concentrated Parabolic Collector (Solar Dish)
EES	Engineering Equation Solver
GWP	Global Warming Potential
HP	Heat Pump
LCC	Life Cycle Cost
ORC	Organic Rankine Cycle
PMV	Predicted Mean Vote
RE	Relative Error
RO	Reverse Osmosis
RSM	Response Surface Methodology
TDS	Total Dissolved Solids
TRNSYS	Transient System Simulation Tool

Symbol Definition Unit

A	Availability factor –
A (subscripted)	Surface area m^2
C_p	Specific heat capacity $kJ\cdot(kg\cdot K)^{-1}$
E_aux	Auxiliary electrical power kW
E_compressor	Compressor electrical power kW
E_control	Control system electrical power kW
E_fan	Fan electrical power kW
E_heat pump	Heat pump electrical power kW
E_pump	Pump electrical power kW
E_RO	Reverse osmosis electrical power kW
E_{cons}	Annual electricity consumption $kWh\cdot year^{-1}$
F_{fuel}	Annual boiler fuel consumption $m^3\cdot year^{-1}$
h	Specific enthalpy $kJ\cdot kg^{-1}$
i	Discount rate –
I_c	Initial capital cost $
LHV	Lower heating value of fuel $kJ\cdot m^{-3}$
M_f	Freshwater production rate $m^3\cdot h^{-1}$
N	Service life year
N_y	Lifetime (years) year
P	Pressure kPa / Pa
PWF	Present worth factor –
Q	Heat transfer rate kW
s	Specific entropy $kJ\cdot(kg\cdot K)^{-1}$
T	Temperature°C
T_a	Air temperature°C
T_{inlet}	Inlet temperature°C
T_{set}	Set/outlet temperature°C
U	Overall heat transfer coefficient $W\cdot(m^2\cdot K)^{-1}$
(UA)_t	Overall heat transfer loss coefficient $W\cdot K^{-1}$
W	Power output / work kW
η	Efficiency %
π	Osmotic pressure Pa

1. Introduction

The accelerating depletion of non-renewable energy reserves represents one of the most critical and urgent challenges confronting the global community. This depletion, coupled with the heavy reliance on fossil fuels, has intensified greenhouse gas (GHG) emissions, accelerated climate change, degraded air quality, and caused significant environmental deterioration, leading to far-reaching socio-economic and ecological consequences [1,2]. In response, a decisive transition toward renewable energy resources—such as solar, wind, geothermal, hydroelectric, and biomass—is essential, as these technologies can meet increasing global energy demand while reducing environmental impacts and creating new economic opportunities in emerging green industries [3]. Among the available renewable options, solar energy stands out due to its global availability, environmental benignity, modular scalability, and applicability across diverse sectors, including electricity generation, space conditioning, water heating, and desalination [4,5]. Recent studies have provided comprehensive energy, exergy, economic and environmental assessments of various solar collector and desalination configurations and highlighted design considerations that enhance thermal efficiency and long-term reliability [5]. These findings strengthen the feasibility of multi-output solar-based systems for residential applications similar to the proposed configuration. Advances in photovoltaic (PV) modules, solar thermal collectors, and hybrid PV/T architectures have significantly enhanced the technical and economic feasibility of solar systems, making them suitable for integrated applications that maximize resource utilization and minimize waste. In recent years, multi-generation systems—capable of simultaneously providing electricity, heating, cooling, and freshwater from a single, integrated renewable platform—have received increasing research and industrial attention [6,7]. Compared with traditional single-output systems, such configurations generally offer higher overall energy and exergy efficiencies, reduced operational costs, and lower environmental footprints [8]. These improvements stem from optimized primary energy use, systematic recovery of waste heat, and integration of energy storage subsystems. Several studies have demonstrated the potential of solar-driven multi-generation systems. Pourmoghadam and Kasaeian (2023) [8] evaluated a parabolic trough collector-based system with phase change material (PCM) storage, identifying toluene as the most effective Organic Rankine Cycle (ORC) working fluid for annual performance. Zheng et al. (2023) [9] proposed a hybrid PV/T–solid oxide fuel cell–electrolysis system achieving an 80.7% energy capture rate and continuous electricity supply for 14 hours. Other notable works include solar–gas turbine integration for hydrogen production [10], biomass–solar hybrid greenhouse systems [11], and solar–geothermal hybrids optimized via particle swarm algorithms [12]. Research has also addressed climate adaptability and hybridization strategies. For example, Wang et al. (2022) [13] developed a TRNSYS-modeled combined cooling, heating, and power (CCHP) system that accounts for weather variability; Hu et al. (2022) [14] analyzed radiant cooling systems under intermittent operation; and Saleem et al. (2020) [15] optimized a hybrid solar–hydrogen generation system using TRNSYS. Additional studies have explored molten salt nanofluids for solar thermal plants [16], PV/wind/fuel cell hybrids with battery storage [17], and integrated systems combining solar energy with ocean thermal energy conversion (OTEC) [18]. Recent research on solar–geothermal hybrid configurations has emphasized optimization under real climatic conditions. For example, a study conducted in ParsaAbad-e-Moghan applied real solar irradiation data to evaluate a combined solar–geothermal system, performing a multi-criteria optimization based on cost, energy, and environmental indicators. The results demonstrated that accurate local solar data can significantly improve both the economic feasibility and energy yield of hybrid renewable systems, highlighting the importance of site-specific analysis in system design [19]. In addition, exergy and cost-based optimization approaches have been employed to enhance complex multi-generation systems integrating compressed air energy storage (CAES), heliostat solar fields, and biomass-fired gas turbine cycles. This combination not only improves dispatchability and reliability but also leverages the complementary characteristics of solar and biomass resources. The integration of CAES further contributes to peak-load management and increases the overall flexibility of the system [20]. Another notable advancement involves the modeling and optimization of hybrid geothermal–solar plants using coupled artificial neural networks (ANN) and genetic algorithms (GA).

Downloaded from https://iranpaper.ir
https://www.tarjomano.com ترجمه تخصصی این مقاله مورد تایید ایران پیپر

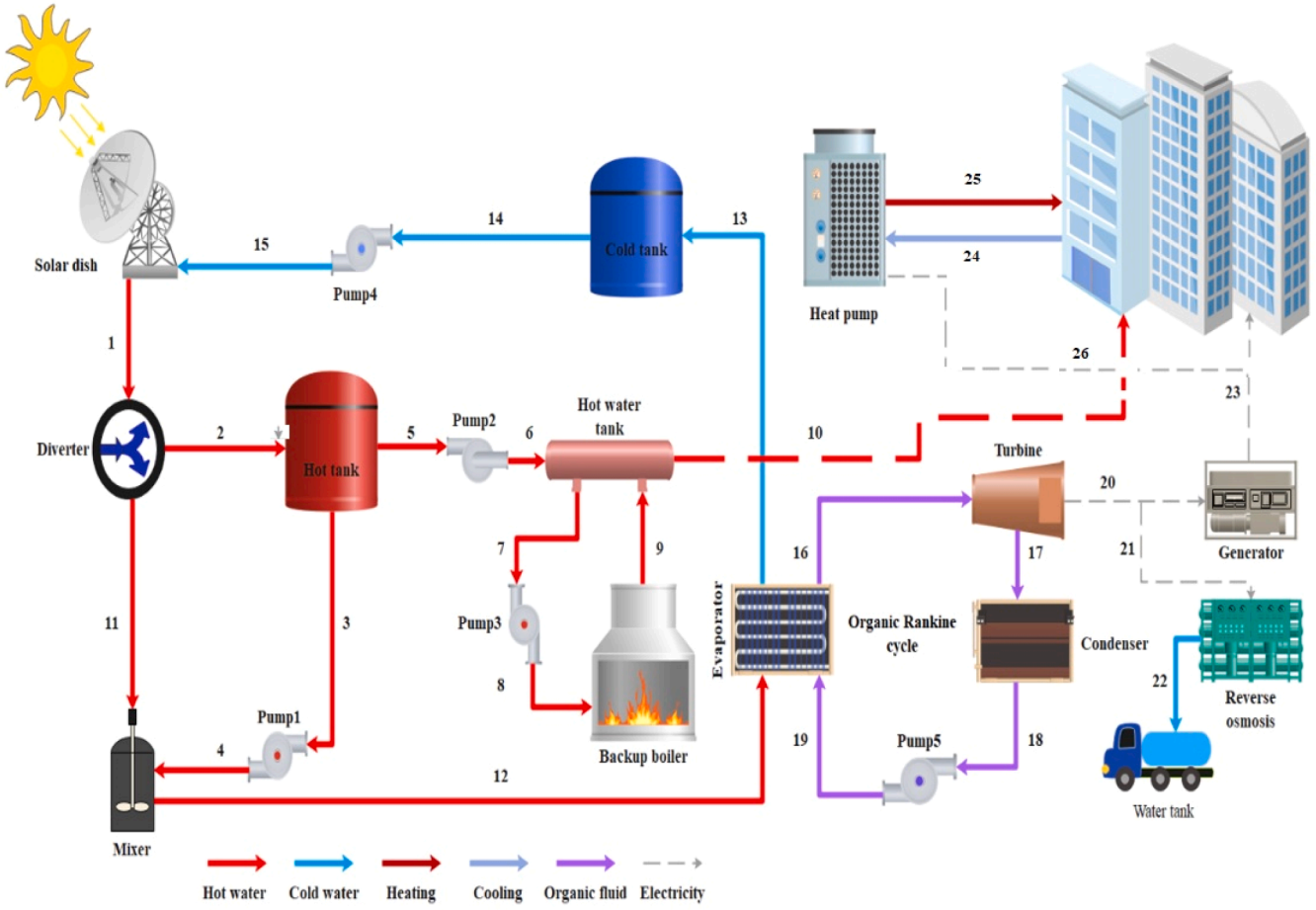

Fig. 1. Schematic of the suggested system.

This method enables accurate prediction of system performance under varying operating conditions and facilitates rapid convergence toward optimal design parameters. By leveraging machine learning alongside evolutionary computation, researchers have achieved substantial improvements in both exergy efficiency and system cost-effectiveness [21]. Furthermore, innovative configurations have been proposed for booster-assisted combined cooling, heating, and power (CCHP) systems based on solar–geothermal energy. Thermoeconomic assessments reveal that incorporating a booster stage can markedly increase system efficiency, reduce primary energy consumption, and enhance the economic return over the system's lifetime. Such designs are particularly promising for regions with simultaneous high heating and cooling demands [22]. Despite these advances, several challenges remain, including maintaining high operational efficiency under seasonal variability, developing standardized multi-objective optimization frameworks that consider technical, economic, and environmental criteria, and unifying simulation platforms for accurate dynamic–thermodynamic performance prediction. To address these gaps, the present study proposes a solar-powered multi-generation system designed to supply annual electricity, heating, cooling, and freshwater for a 100-unit residential complex in Tehran, Iran. The configuration integrates a solar dish concentrator, ORC, heat pump, reverse osmosis desalination unit, hot and cold water storage tanks, and an auxiliary boiler [23]. Dynamic simulations are performed in TRNSYS, thermodynamic modeling in EES, and multi-objective optimization via Response Surface Methodology (RSM), targeting minimized life cycle cost, boiler fuel consumption, and electricity demand while maximizing thermal comfort. The study also introduces a dimensionless scaling methodology, enabling adaptation of the proposed system to diverse climatic contexts without full re-simulation, thereby enhancing its replicability and market potential. Building on these advances, this study proposes an innovative solar-powered cogeneration system capable of supplying the annual electricity, heating, cooling, and freshwater demands of a 100-unit residential complex in Tehran, Iran. The proposed configuration uniquely integrates a solar dish concentrator, Organic Rankine Cycle (ORC), heat pump, and reverse osmosis desalination unit within a unified framework, modeled through the combined use of TRNSYS and EES environments.

The novelty of this work is fourfold:

1. Integrated modeling approach – Coupling TRNSYS dynamic simulations with EES thermodynamic analysis to capture both transient and steady-state system behavior.
2. Multi-objective optimization – Employing Response Surface Methodology (RSM) to simultaneously minimize life cycle cost (LCC), boiler fuel consumption, and electricity demand while maximizing thermal comfort as quantified by the Predicted Mean Vote (PMV) index.
3. Working fluid evaluation – Conducting a comparative analysis of conventional and emerging ORC working fluids with respect to thermodynamic efficiency, environmental impact, and operational compatibility.
4. Scalable design methodology – Introducing a dimensionless scaling approach that enables rapid adaptation of the proposed system to diverse climatic conditions without the need for complete re-simulation.

Accordingly, the specific objectives of this research are to:

Downloaded from https://iranpaper.ir
https://www.tarjomano.com ترجمه تخصصی این مقاله مورد تایید ایران پیپر

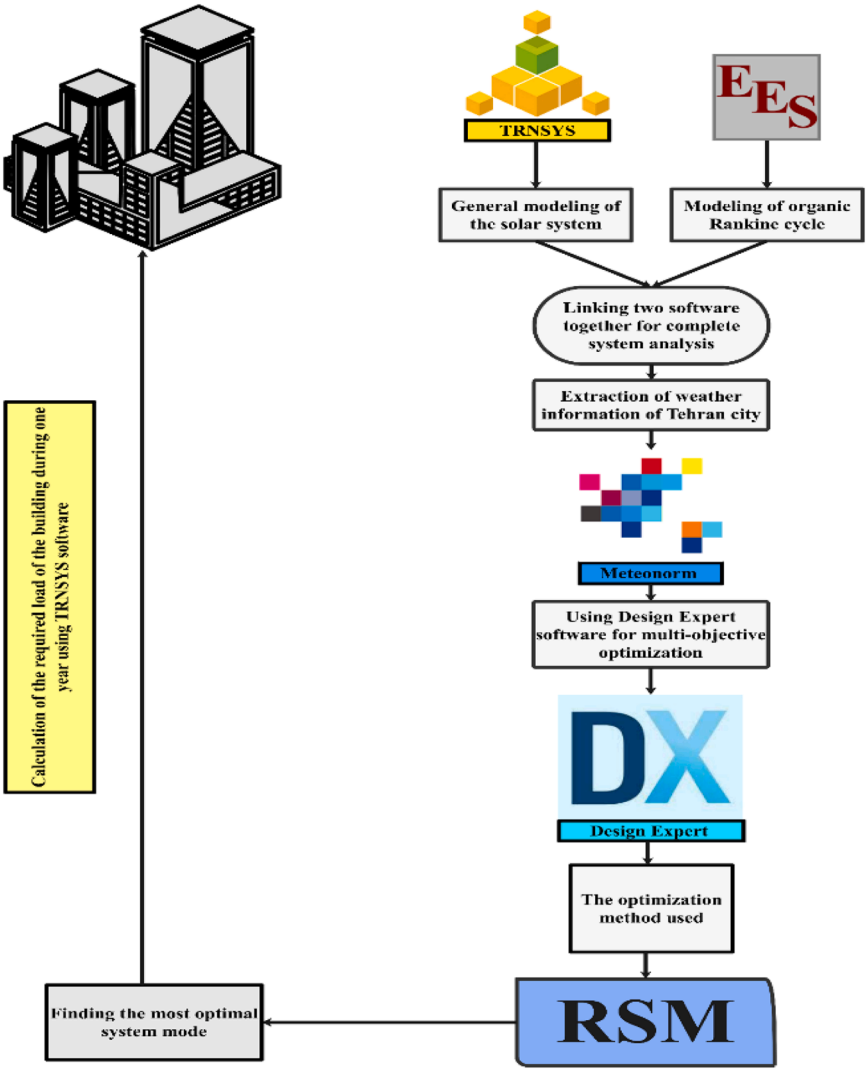

Fig. 2. Research methodology.

- Determine the optimal operational conditions for the proposed cogeneration system under local climatic constraints.
- Quantify technical, economic, and environmental performance improvements relative to conventional single-generation systems.
- Assess the system's capacity for CO_2 emissions reduction and compliance of produced freshwater with WHO quality standards.
- Develop design guidelines that facilitate system deployment in various climatic zones.

By fulfilling these objectives, this study aims to bridge the gap between theoretical modeling and practical implementation of renewable multi-generation systems, contributing to enhanced energy autonomy, environmental sustainability, and cost-effective resource utilization in residential applications.

2. Overview of the system

The architecture of the proposed renewable energy system, illustrated in Fig. 1, comprises several essential components, including a solar dish, a heat pump, an organic Rankine cycle (ORC), hot and cold thermal storage units, a steam boiler, a domestic hot water storage tank, and a reverse osmosis (RO) desalination unit. A utility grid connection is incorporated as a critical backup due to the intermittent nature of solar energy. This connection ensures system stability by supplying energy during periods of insufficient solar input and by accommodating surplus power generation when available. In operation, the solar dish collects solar radiation and transfers the absorbed energy to a heat transfer fluid, raising its temperature. The heated fluid is stored in the hot thermal storage unit, from which part of the thermal energy is directed to the ORC evaporator. In the ORC, the working fluid is vaporized in the evaporator, driving the turbine to produce electricity. The hot storage unit also supplies thermal energy through a diverter to meet domestic hot water demands. This heat is transferred to a water heater, which delivers hot water to the target residential units. An auxiliary boiler is integrated into the circuit to provide additional thermal energy when both solar input and stored heat are insufficient to meet demand. The thermal cycle is completed when the cooled fluid, after releasing its energy in the water heater or ORC, returns to the cold storage tank and is recirculated to the solar dish via a circulation pump. The RO desalination unit, powered by electricity generated from the ORC turbine, removes salts and impurities from seawater or brackish water to produce potable water. The heat pump is another key subsystem, delivering both space heating and cooling with minimal electricity consumption relative to the system's total output. Once the energy needs of the residential buildings and all system components are satisfied, any surplus electricity is exported to the national grid. This integrated configuration leverages multiple renewable energy conversion pathways—solar thermal, thermodynamic cycles, thermal storage, and desalination—to deliver

iranpaper Downloaded from https://iranpaper.ir
https://www.tarjomano.com ترجمه تخصصی این مقاله مورد تایید ایران پیپر

Table 1
Design specifications of apartment units.

Parameter	Value	Unit
Building area	190	m^2
Window number	2	m^2
Window area	3	-
heat coefficient	3	$\frac{W}{m^2 K}$
Roof heat	0.29	$\frac{W}{m^2 K}$
RoofSolar absorptance	0.5	-
Wallsheat transfer coefficient	0.6	$\frac{W}{m^2 K}$

Table 2
Specifications of loads inside residential units.

Gain	Ceiling height	Convective	Electric power fraction	Abs. humidity
People	72	144	0	0.059
Electrical	14904	4968	1	0
Lights	388	166	1	0

electricity, space heating and cooling, domestic hot water, and freshwater. The design exemplifies a sustainable, multifunctional approach to renewable energy utilization, optimizing resource use while enhancing energy resilience for residential applications.

2.1. Research methodology

Fig. 2 shows the flowchart illustrating the problem-solving approach in this study.

2.2. System modeling

The proposed system is designed applying a combination of two powerful software tools:

1. TRNSYS (Transient System Simulation Tool): TRNSYS is a versatile and robust simulation tool specifically designed for energy systems in transient states [24]. It is built on FORTRAN programming language, allowing for precise modeling and analysis of dynamic systems.
2. EES (Engineering Equation Solver) is a powerful programming tool for solving algebraic and transcendental equations related to thermodynamics and fluid mechanics [25]. It provides built-in thermophysical property functions for a wide range of fluids, as well as numerical algorithms that allow simultaneous solution of nonlinear systems of equations. In the present study, EES was employed to model the proposed hybrid system and to solve the complete set of governing equations presented in Section 3. The software enabled the iterative calculation of state properties, mass and energy balances, and performance parameters of each subsystem (solar dish, heat pump, ORC, and RO). Moreover, EES facilitated sensitivity analyses by varying design and operational parameters, ensuring both accuracy and computational efficiency in predicting the overall performance of the integrated configuration.These features make EES particularly suitable for analyzing complex energy systems in which multiple components are thermodynamically coupled.

2.2.1. Building

This research involved the evaluation of a theoretical scenario in which 100 housing units were projected to be located in ten structures. Two residential units were located on each of the five levels of each of these structures. The specifications and characteristics of residential units within the complex are comprehensively detailed in Table 1.

Table 2 displays data on the humidity levels produced by the individuals in the building, the amount of light present, and the number of electrical devices. This data is essential for precisely modeling and achieving genuine findings for parameters such as the proportions of radiative, convective, and electric power inside the building.

2.2.2. Solar dishes

In order to collect solar energy, this research used a solar dish receiver. With a solar dish receiver system, parabolic dishes that constantly modify their orientation to correspond with the sun's position are used to direct sunlight toward the focal point. These dishes usually align properly with tracking systems [26]. Advanced receiver designs, such as corrugated or twisted geometries, as reported in recent experiments by Rawa, M. J., et al. These approaches are in line with the goals of system scalability and performance improvement of the present work [27].

The useful thermal energy gained by the collector is obtained from the energy balance:

$$Q_u = A_{ap} \cdot I_{solar} \cdot \eta_{opt} - Q_{loss}$$

where:

- A_{ap} is the aperture area of the dish [m^2],
- I_{solar} is the solar irradiance[W/m^2],
- η_{opt} is the optical efficiency of the concentrator,
- $Q_{loss} = U \cdot A_{ap} \cdot (T_{col} - T_{amb})$ represents thermal losses.

2.2.3. Heat pump

TRNSYS software with a customized database was applied to integrate and control the heat pump system, which was used to meet the building's energy needs unit analysis.

The following equation can be used to identify the production power of the organic Rankine cycle [28]:

$$\dot{W} = \dot{m_{in}} \left(W_{turbine} - W_{pump} \right) \quad (1)$$

$$\dot{W_{turbine}} = \dot{m_{16}} \left(h_{17} - h_{16} \right) \quad (2)$$

$$\dot{W_{pump}} = \dot{m_{18}} \left(h_{19} - h_{18} \right) \quad (3)$$

These equations represent power, mass flow rate, and enthalpy.

2.2.4. Thermal energy storage unit analysis

Solar thermal energy storage systems are essential for satisfying a building's energy requirements. They do this by absorbing and preserving the sensible heat of molten salt, which enables efficient and dependable energy storage [29,30].

$$\frac{dM}{dt} = \dot{m_{in}} - \dot{m_{out}} \quad (4)$$

$$C_p \times \frac{d(MT)}{dt} = \dot{m_{in}} C_p T_{in} - \dot{m_o} C_p T - (UA)_t (T - T_a) \quad (5)$$

The quantity M shows the instantaneous mass of heat transfer fluid in the tank in the equations above. Moreover, T stands for the fluid temperature in the storage tank, Cp stands for the specific heat capacity, and (UA)t overall heat transfer loss coefficient. Also, Hakan F. Öztop et al. showed in PCM-based storage systems that geometric modifications in the heat exchanger components in the storage unit can significantly increase the freezing rate and discharge efficiency [31]. These findings are relevant for improving the performance of hot and cold-water storage in our proposed design.

iranpaper Downloaded from https://iranpaper.ir
https://www.tarjomano.com ترجمه تخصصی این مقاله مورد تایید ایران پیپر

Table 3
Coefficients for freshwater rates.

Coefficients	A_1	A_2	A_3	B_1
Value	0.067	184	129	868

Table 4
Design parameters of evaporator and condenser units (data adapted from [41, 43] and assumptions in this study).

Parameter	Symbol	Amount
Turbine efficiency	$\eta_{ise,T}$	*0.85 %*
Pump efficiency	$\eta_{ise,P}$	*0.85 %*
$Condenser_{efficiency}$	η_{con}	*0.85 %*
Condenser outlet temperature	$T_{out,con}$	*50 °C*
Condenser outlet pressure	$P_{out,con}$	*100 kPa*
EvaporatorPinch point temperature	$\Delta T_{eva,pp}$	*20 °C*
CondenserPinch point temperature	$\Delta T_{con,pp}$	*20 °C*

2.2.5. Reverse osmosis unit modeling

The reverse osmosis (RO) subsystem is powered by electricity generated from the ORC turbine. Its purpose is to produce freshwater from saline feedwater, with quality assessed based on total dissolved solids (TDS). The unit's performance is estimated using empirical correlations from [32–34].

The net pump power requirement for the RO system is given by

$$Pump_{Power} = \left(\dot{W}_{net,ORC} + \dot{W}_{TEG,wp}\right) \times 1.79 \tag{6}$$

The rate of fresh water is obtained from the following equation:

$$FreshWaterRate = \frac{A_1 \times PumpPower^2 + A_2 \times PumpPower + A_3}{PumpPower + B_1} \tag{7}$$

Equations (6) and (7) describe the freshwater yield and energy consumption of the RO unit. In the RO process, the net driving force for water flow through the semipermeable membrane is given by (ΔP - π), where ΔP is the applied hydraulic pressure and π is the osmotic pressure of the feed (brine) solution. Osmotic pressure is calculated as:

The specific energy consumption of the RO unit is:

$$E_{RO} = \frac{W_{pump}}{\dot{m}_{fw}} \tag{8}$$

The net freshwater production rate is obtained as:

$$\dot{m}_{fw} = \dot{m}_{in} \cdot (1 - r) \tag{9}$$

$$\pi = i \cdot R \cdot T \cdot C \tag{10}$$

where i is the van't Hoff factor, R the universal gas constant, T the absolute temperature, and C the molar concentration of dissolved salts. As brine concentration increases, π increases, reducing the effective driving pressure (ΔP - π) and thus lowering freshwater flux. Hence, the freshwater production modeled in Eq. (6) depends not only on ΔP but also on π, which links the yield directly to brine concentration. Similarly, energy consumption in Eq. (7) is influenced by the pump power required to overcome both osmotic pressure and hydraulic losses.

This connection aligns with literature findings that emphasize that high salinities demand higher applied pressures due to increased osmotic pressure [35,36]. freshwater production is measured in cubic meters per hour. Table 3 shows this study measures freshwater production.

Material innovations in reverse osmosis membranes, such as positively charged polyamide layers or nanocomposite coatings, have been shown by Azman, M. A. N., et al to improve salt rejection, fouling resistance, and radionuclide removal [37]. These advances provide valuable insights into the selection and optimization of RO components for integration into solar multigeneration systems.

In this study, the modeled RO unit achieves freshwater TDS levels below 500 mg/L, meeting WHO drinking water standards. The RO subsystem is thus capable of providing potable water while operating within the integrated cogeneration system.

2.2.6. Boiler

The auxiliary steam boiler supplies thermal energy to the water heater whenever solar heat and hot water storage are insufficient. Boiler performance is modeled according to ASHRAE standards [38,39].

$$\dot{Q}_{need} = \dot{m}_{fluid} C_{p,fluid} (T_{set} - T_{in}) \tag{11}$$

$$PLR = \frac{\dot{Q}_{need}}{\dot{Q}_{max}} \tag{12}$$

$$T_{out} = T_{in} + \frac{\dot{Q}_{max}}{\dot{m}_{fluid} C_{p,fluid}} \tag{13}$$

Boiler fuel consumption; studying fresh water product from the device by:

$$\dot{Q}_{exhaust} = \dot{Q}_{fluid} (1 - \eta_{combustion}) \tag{14}$$

The energy lost during the combustion process by:

$$\dot{Q}_{loss} = \dot{Q}_{fluid} - \dot{Q}_{exhaust} \tag{15}$$

2.2.7. Storage Tanks

The thermal balance of the storage tank is expressed as:

$$m \cdot c_p \cdot \frac{dT}{dt} = \dot{Q}_{in} - \dot{Q}_{out} - (UA)_t (T - T_{amb}) \tag{16}$$

where $(UA)_t$ is the overall heat transfer loss coefficient.

As shown in Table 4, the pinch point temperature difference is assumed to be 20°C for both evaporator and condenser. This value is considerably higher than what is commonly used in ORC heat exchanger design, where many studies report pinch point differences in the range of 5–15°C for evaporators and condensers under realistic operating conditions (e.g. Sun et al. 2018 [40], Jin et al. 2020 [41]). The higher pinch point assumed in this study is due to simplifying assumptions in the heat exchanger modeling and to account for unforeseen thermal losses and irreversibilities. In practice, using a lower pinch point (e.g. ~ 10°C) could reduce thermal losses and improve cycle efficiency, though it may necessitate larger heat exchanger area and higher capital cost (Bett et al. 2021 [42]). The assumption in this work (20°C) therefore delineates a more conservative estimate of performance.

The effect of organic fluids on the performance of the organic Rankine cycle was investigated as a crucial factor affecting the overall system's efficiency. Fig. 3 illustrates the flowchart of the comprehensive process for solving and optimizing the problem.

2.3. Economic analysis

As part of the economic analysis of the proposed solar system, this study employs a comprehensive approach to evaluate its annual cost over the entire service life. The annual cost includes the capital recovery portion of the initial investment, equipment replacement costs, and all other recurring expenses, such as those associated with system operation, monitoring, control, and performance optimization. These costs are assessed over a 25-year operational period, providing a realistic estimate of the long-term financial commitment required to maintain and operate the solar system efficiently.

2.4. Response surface method (RSM)

The technical and financial performance of the proposed system is

iranpaper Downloaded from https://iranpaper.ir
https://www.tarjomano.com ترجمه تخصصی این مقاله مورد تایید ایران پیپر

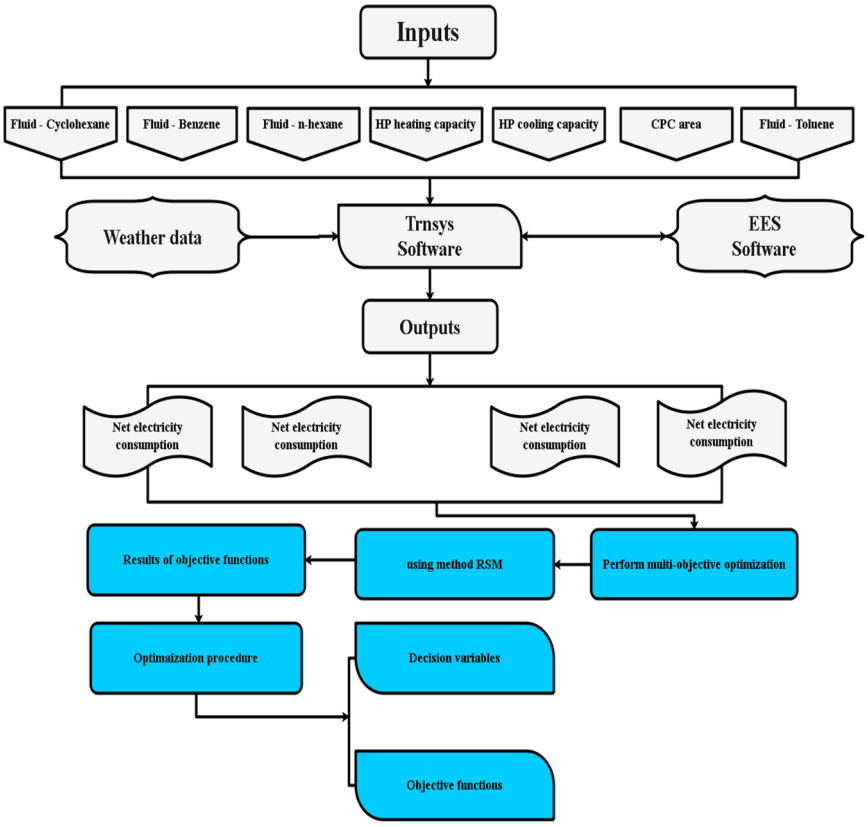

Fig. 3. Flowchart of research.

Table 5
Decision variables.

Name	Lower bound	Upper bound	Unit
CPCarea	0	300	m^2
HP cooling capacity	0	100	kW
HP heating capacity	0	100	kW
fluid – Toluene	Categoric factor	Categoric factor	-
fluid - n-hexane	Categoric factor	system's inputs and outputs	-
fluid – Benzene	Categoric factor	Categoric factor	-
fluid – Cyclohexane	Categoric factor	Categoric factor	-

Table 6
Validation results of the proposed model (all variables are defined below and in the Nomenclature section).

Symbol	Definition	Unit	Reference [49]	Current study	Difference (%)
-	Turbine power output	kW	1131	1122	0.79
M_f	Freshwater production rate	$m^3 \cdot h^{-1}$	485	485	0
-	RO freshwater flow rate	$m^3 \cdot h^{-1}$	0.9	0.9	0
E_cons	Annual electricity consumption	$kWh \cdot year^{-1}$	64180	64180	0
LCC	Life cycle cost	$	250	252	0.8
-	Pump power consumption	kW	6850	6856	0.08

enhanced by incorporating these costs into a multi-objective annual cost framework, evaluated using the Response Surface Methodology (RSM). This approach involves designing a cost-effective set of experiments to

Table 7
Validation of ORC Cogeneration Subsystem with Experimental Data.

Parameter	Experimental Value	Present Study	Difference (%)
ORC turbine outlet temperature (°C)	155.0	151.8	2.06
Net electrical power output (kW)	21.5	21.1	1.86
Freshwater production rate (m^3/h)	0.92	0.90	2.17

Table 8
Optimal results of Decision variables and optimizations.

Decision variables	CPC area (m2)	$HP_{cooling\ capacity}$, (kW)	$HP_{heating\ capacity}$, (kW)	Fluid type
Optimum	101.251	20.27	36.294	Benzene
Objective functions	Electricity consumption (kWh/year)	Boiler fuel consumption (m^3/year)	PMV	LCC ($)
Optimum	6437.4	6918.004	0.26	134130

assess the process performance and determine additional cost components, including those related to operation, monitoring, and key system variables. Through this optimization technique, the contribution of each factor to the overall system performance is quantified, enabling a balanced trade-off between technical efficiency and economic feasibility. Table 5 presents the seven key influencing factors considered in the analysis. These cost-related and operational parameters were selected to optimize the objective functions and assess the system's technical and financial outcomes. The response surface optimization process was conducted using Design-Expert software, which

iranpaper Downloaded from https://iranpaper.ir
https://www.tarjomano.com ترجمه تخصصی این مقاله مورد تایید ایران پیپر

Table 9
Comparative assessment of candidate ORC working fluids.

Fluid	Thermo performance (literature trend)	Environmental (ODP / GWP100)	Safety / Classification	Notes (practicality)
Benzene	Often high efficiency at medium–high source T in parametric studies [55]	ODP≈0 / GWP≈0 (hydrocarbon).	Flammable; high chronic toxicity; IARC Group 1 carcinogen.	Regulatory and HSE constraints limit practical deployment.
Toluene	Frequently among top performers; high η in regenerative/recuperated ORCs [55,56].	ODP≈0 / GWP≈0 (hydrocarbon).	Flammable; moderate toxicity; widely reported for high-T ORCs [57]	Thermally stable at higher T with proper materials; common in literature.
R1233zd(E)	Good efficiency for low- to medium-T sources; slightly lower than aromatics in some cases [56]	ODP≈0 / GWP≈1 (ultra-low) [56]	ASHRAE A1 (non-flammable); favorable safety profile.	Commercial availability; ORC demonstrations reported [56]
Cyclohexane	Comparable/competitive with toluene in some bottoming ORCs [55]	ODP≈0 / GWP≈0 (hydrocarbon).	Flammable; lower toxicity than benzene (still handle per HSE).	Attractive thermodynamics; safety controls required.

systematically analyzes the interaction effects of these factors to identify optimal operating conditions.

Optimizing the and assessing system's technical and financial performance. The response-level functions, estimated average value of votes, life cycle cost, electricity consumption, and boiler fuel consumption. References to other sources [44–46] may provide more detailed information or methods to develop these objective functions.

$$OEC = \frac{\sum_{i=1}^{n}\left(E_{load,prof,i} + E_{exp} + E_{microexp} + E_{pump,i} + E_{compressor} - E_{PV,T} - E_{fuel,cell} - E_{TP}\right)}{3600 \times \frac{1}{\Delta t}} \quad (17)$$

$$BFC = \frac{\sum_{i=1}^{n}\left(\dot{m}_i\, c_p\, \left(T_{supply,i} - T_{return,i}\right) f_{boiler}\right)}{\eta_{boiler}\, LHV} \quad (18)$$

$$PMV = 0.3{\cdot}\exp(-0.036M) + 0.02{\cdot}L_E \quad (19)$$

$$LCC = I_c + PWF{\cdot}AOC - R_t \quad (20)$$

$$PWF = \frac{1 - \left(\frac{1+i}{1+d}\right)^{n_L}}{d - i} = \frac{n_L}{1+d} \quad (21)$$

In Eq. (13), as can be seen, the overall electricity consumption (OEC) is calculated as the sum of the electrical energy demands of all major components in the system, including the heat pump ($E_{heat\ pump}$), fans (E_{fan}), water pumps (E_{pump}), compressor ($E_{compressor}$), reverse osmosis desalination unit (E_{RO}), control systems ($E_{control}$), and any auxiliary devices (E_{aux}). The summation is performed over the operational periods of these devices, and the total value is normalized by the annual operating hours. The multiplication factor $\times\ 3600 1/A$ is used to convert the instantaneous power values into annual energy consumption in kilowatt-hours per year (kWh/year), where A denotes the system availability factor. This equation provides a comprehensive measure of the electrical performance of the cogeneration system and serves as a key indicator for estimating operational costs, evaluating environmental impacts, and optimizing overall system efficiency. In Eq. (14), as can be seen, the boiler fuel consumption (BFC) is determined based on the thermal energy required to raise the temperature of the working fluid from the inlet temperature (T_{inlet}) to the set outlet temperature (T_{set}) for each operating period i. This energy is divided by the boiler efficiency and the lower heating value (LHV) of the fuel to determine the actual fuel consumption in cubic meters per year (m^3/year). This equation is essential for quantifying fuel usage, estimating operating costs, and assessing the environmental impact of the system.

In Eq. (15), as can be seen, the Predicted Mean Vote (PMV) is calculated to evaluate the thermal comfort conditions experienced by occupants within the conditioned space. The equation relates environmental parameters such as air temperature (T_a), humidity, and human factors to a dimensionless comfort index ranging from –3 (cold) to +3 (hot), with zero representing neutral comfort. In Eq. (16), as can be seen, the Life Cycle Cost (LCC) is calculated as the sum of the initial capital investment (I_c) and the product of the Present Worth Factor (PWF), the annual operation and maintenance costs (AOC), and the lifetime of the system in years (N_y). The PWF is a dimensionless factor used to convert a uniform annual series of costs into its present value, taking into account the discount rate (i) and the system's service life (N).

3. Model Validation with Experimental and Literature Data

Similar thermodynamic and transient validation approaches have been reported by Afshar, S., et al for solar-ORC systems, where the modeled outputs are cross-validated with experimental datasets and established simulation benchmarks [47]. This strengthens the confidence in the integrated TRNSYS-EES modeling framework used here. To ensure the robustness and reliability of the simulation outcomes, the integrated TRNSYS–EES model was validated using both experimental data reported in the literature and previously published simulation benchmarks for comparable solar-powered ORC-based cogeneration systems. The validation procedure comprised two main stages:

1. Validation of the ORC-based cogeneration subsystem:

Key thermodynamic and operational parameters, including turbine outlet temperature, net electrical power output, and freshwater production rate, were compared with experimental measurements from [48] and an additional independent experimental source.

2. Validation of the reverse osmosis (RO) desalination subsystem:

The RO model was validated against the empirical performance data reported by Nafey and Sharaf (2010) [49], which studied a solar–ORC–RO integrated system. The assessment covered freshwater mass flow rate, total dissolved solids (TDS), electricity consumption of the RO pump, and life cycle cost (LCC).

Table 6 presents the validation results of the proposed hybrid model against reference data reported in [49]. The variables are defined as follows: M_f – freshwater production rate ($m^3{\cdot}h^{-1}$), E_cons – annual electricity consumption ($kWh{\cdot}year^{-1}$), LCC – life cycle cost ($). Additional rows correspond to turbine power output (kW), RO freshwater flow rate ($m^3{\cdot}h^{-1}$), and pump power consumption (kW). All variables are defined in the Nomenclature section for clarity. As can be observed, the results of the current study are in excellent agreement with the reference values, with relative errors below 1% for all parameters, which confirms the accuracy and robustness of the developed model Table 7.

iranpaper Downloaded from https://iranpaper.ir
https://www.tarjomano.com ترجمه تخصصی این مقاله مورد تایید ایران پیپر

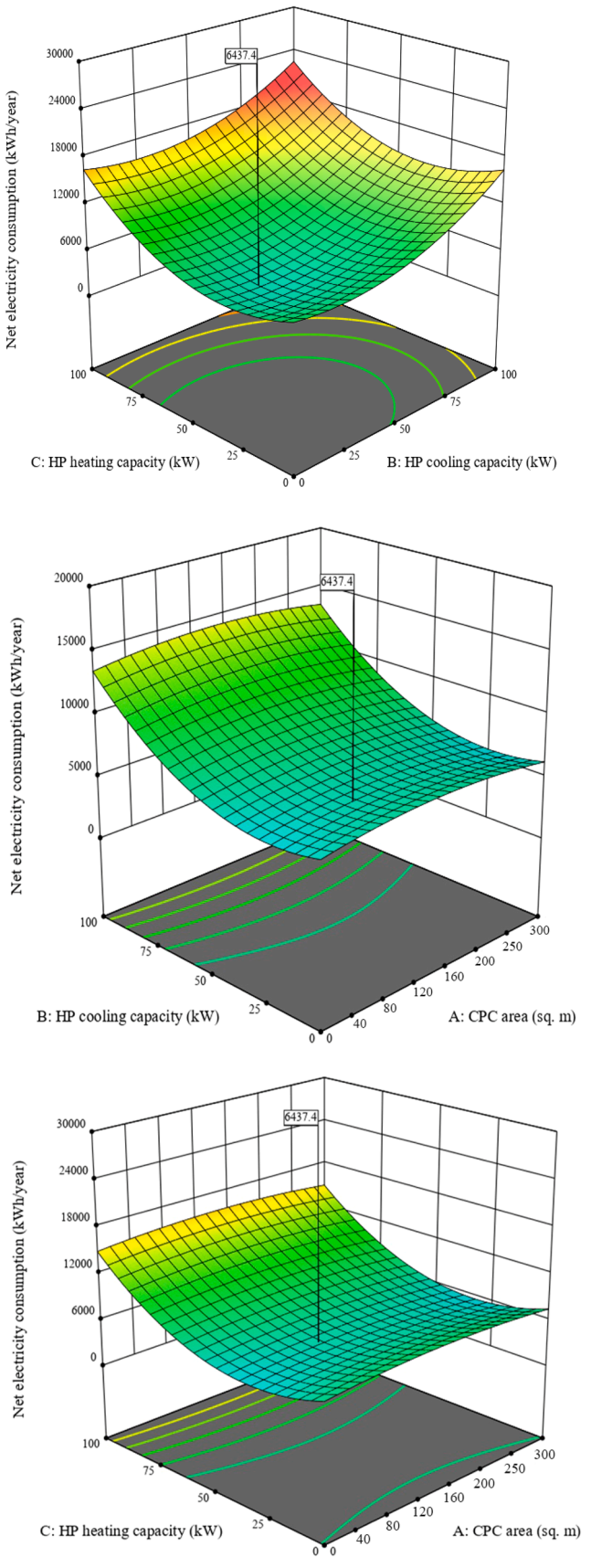

Fig. 4. Mutual effects of design variables on produced electricity.

The validation results indicate that all relative errors were below 3%, which is well within the accepted tolerance for transient simulations of renewable energy systems.

Key findings from the validation are as follows:

- Thermal and electrical outputs of the ORC subsystem matched experimental results with deviations under 2.1%, confirming the accuracy of the thermodynamic modeling.
- Freshwater production rates were reproduced with deviations under 2.2%, with the modeled TDS consistently below 500 mg/L, meeting WHO drinking water standards.
- Economic metrics such as LCC and electricity consumption for the RO unit showed less than 1% deviation from reference values, validating the economic model integration.

By incorporating validation at both the subsystem and system levels, this study ensures that the proposed TRNSYS–EES–RSM framework delivers credible, reproducible, and technically sound results, which enhances confidence in its application to design, optimization, and scalability studies for various climatic conditions

4. Optimization results

The response surface methodology (RSM) was effectively implemented to optimize four meticulously chosen objective functions in order to accomplish the system's optimal technical and economic performance [50]. Ultimately, this method enabled the identification of the most optimal values for the objective functions and the decision variables, resulting in the optimal configuration of the system's operating conditions.

Throughout the optimization process, the following assumptions were made:

- The target city for the study was Tehran.
- The economic analysis considered a system lifespan of 20 years.
- The electricity purchase rate from the network was assumed to be \$0.018 per kWh, and to achieve this, the network was assumed to be \$0.015 per m^3 of gas.

The response surface method was employed to identify 100 optimal points for four objective functions and seven decision variables from 35 simulation results. The optimization approach ultimately determines that Point 1 is the optimal option for identifying the system's appropriate performance. The results of this optimization are presented in Table 8.

4.1. Discussion on working fluid selection and comparison with emerging ORC fluids

The optimization results (Table 8) identify benzene as the optimal working fluid for the overall performance objectives—namely electricity consumption, boiler fuel consumption, PMV, and LCC—under Tehran's climate and load profile. Notably, while toluene shows higher thermodynamic cycle efficiency during initial analyses, benzene offers a better overall balance between efficiency, cost, and component sizing, particularly for medium-temperature operation—consistent with prior findings [51]. Although benzene exhibits favorable thermophysical properties—such as lower viscosity, suitable boiling point, and higher thermal stability—its associated toxicity and safety concerns cannot be overlooked. Thus, in practical applications, selecting a slightly less efficient but safer alternative, like toluene or cyclohexane, may be warranted depending on local safety regulations and project priorities [52]. To explore greener alternatives, the performance of low-GWP fluids was also considered. Hydrofluoroolefins (HFOs), particularly R1233zd(E), have shown promising performance in ORC systems, offering comparable or slightly lower thermal efficiencies but significantly

Downloaded from https://iranpaper.ir
https://www.tarjomano.com ترجمه تخصصی این مقاله مورد تایید ایران پیپر

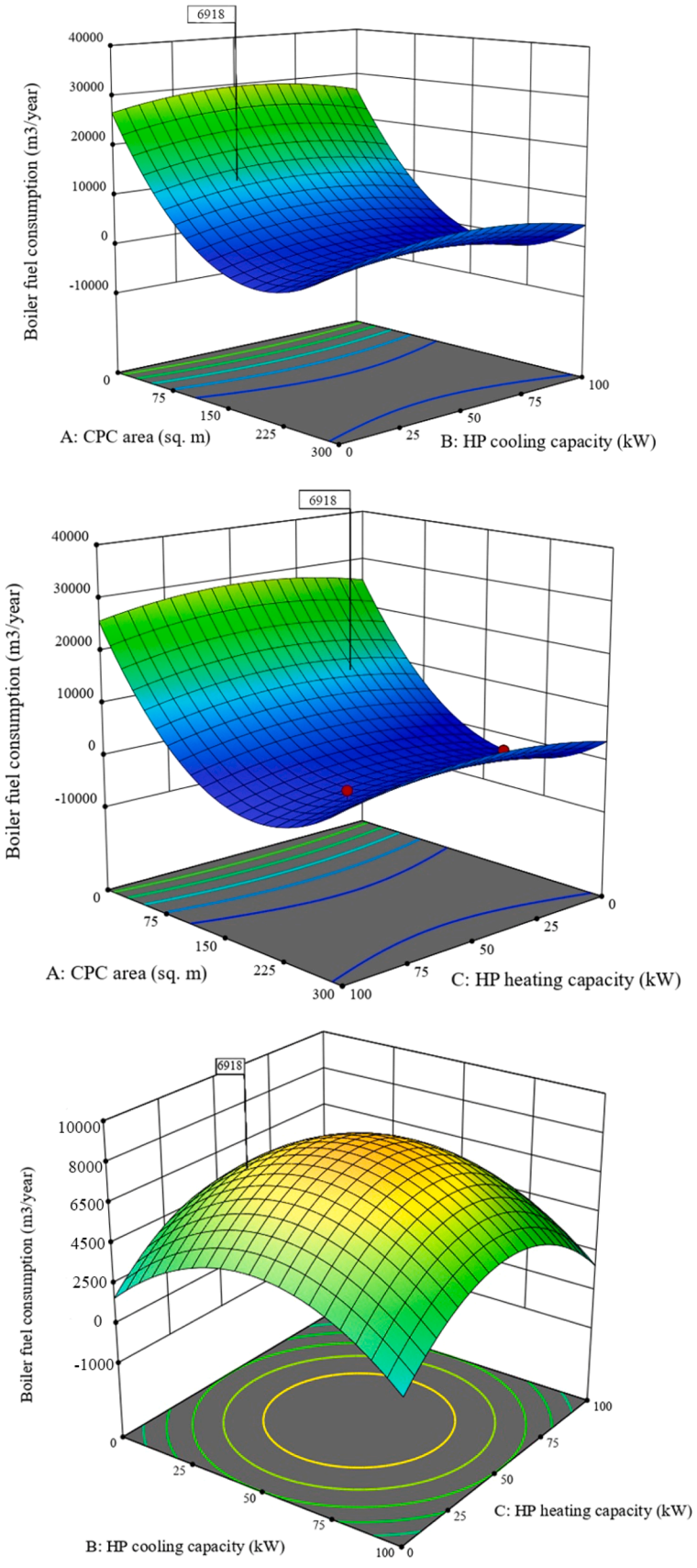

Fig. 5. The effect of changes in design parameters on changes in fuel consumption.

Downloaded from https://iranpaper.ir
https://www.tarjomano.com ترجمه تخصصی این مقاله مورد تایید ایران پیپر

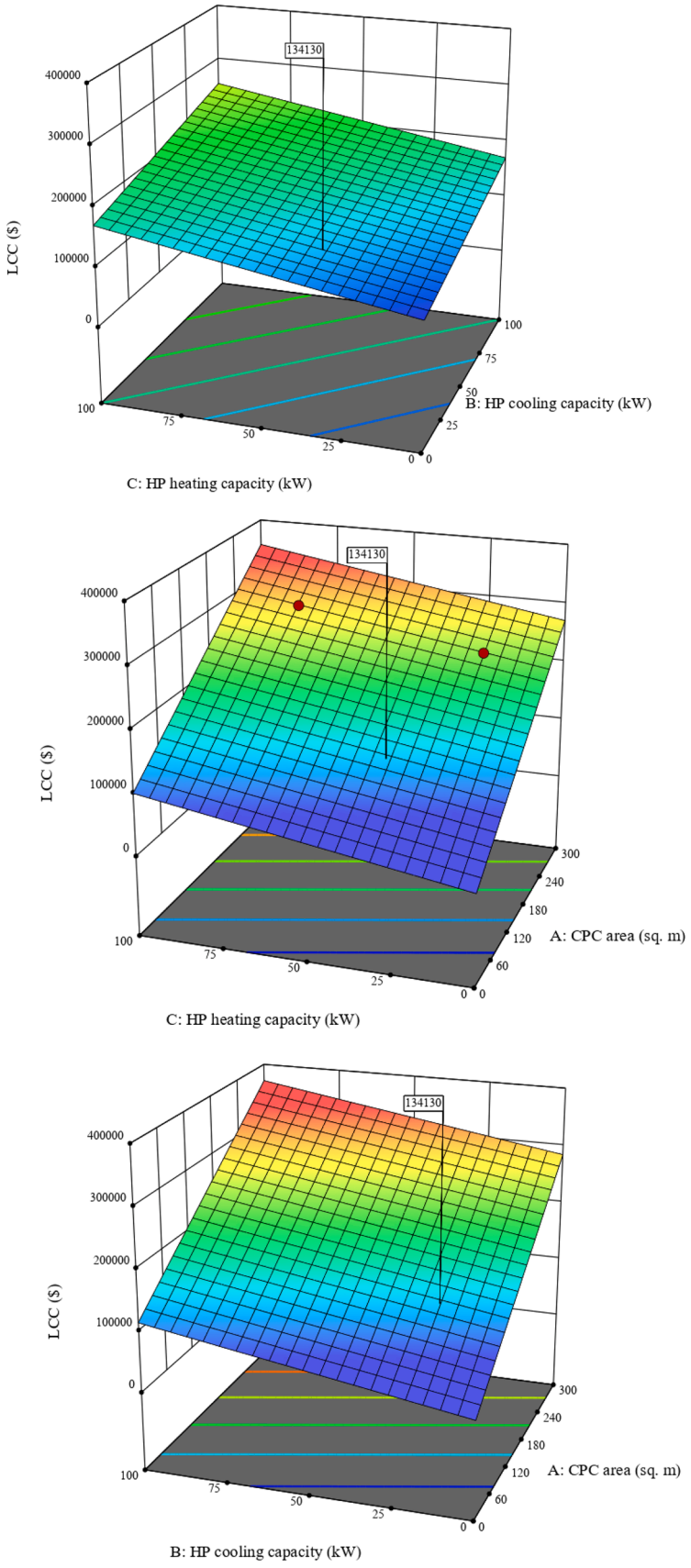

Fig. 6. interaction between design parameters and variations in life cycle cost.

Downloaded from https://iranpaper.ir
https://www.tarjomano.com ترجمه تخصصی این مقاله مورد تایید ایران پیپر

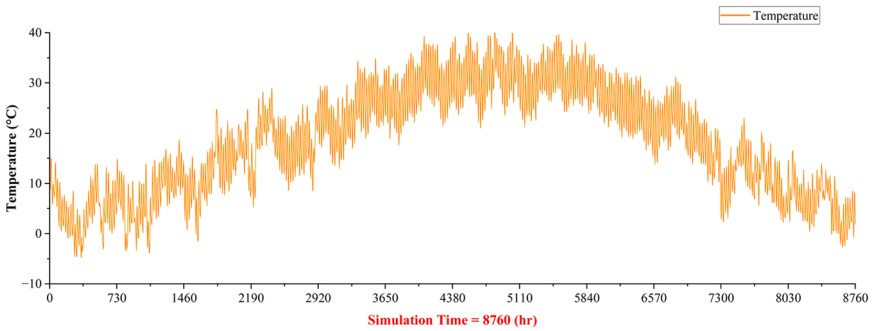

Fig. 7. Hourly ambient temperature of Tehran city throughout the year.

reduced environmental impact and improved safety categorization. One study demonstrated that R1233zd(E) delivered a 6.2% thermal efficiency in a waste heat recovery application while featuring zero GWP [53]. Thermo-economic assessments further indicate that R1233zd(E) offers a better overall performance index compared to traditional R245fa, with only a ~2.3% increase in specific investment cost [54]. Preliminary comparative analyses suggest that replacing benzene with R1233zd (E) in our system setup could result in a modest reduction (approx. 3–5%) in cycle efficiency, while substantially lowering environmental impact. This trade-off underscores the importance of multi-criteria decision frameworks in selecting ORC fluids for real-world implementations. In conclusion, benzene may remain optimal within the confines of our current multi-objective framework, but for large-scale, long-term deployments—especially where environmental compliance and operational safety are paramount—alternatives like R1233zd(E) or cyclohexane present compelling and responsible alternatives. For clarity, a comparative summary of the four candidate fluids (benzene, toluene, R1233zd(E), and cyclohexane) in terms of efficiency, safety, and environmental impact is presented in Table 9.

Based on our optimization objective and the modeled source/sink conditions, benzene emerged as the mathematically optimal fluid in terms of cycle efficiency. However, considering safety (carcinogenicity and flammability) and environmental compliance, R1233zd(E) and toluene represent more practical choices for implementation. In particular, R1233zd(E) combines acceptable thermodynamic performance with ASHRAE A1 (non-flammable) classification and ultra-low GWP (≈1), which can simplify permitting and HSE risk management without severely compromising efficiency [56].

Fig. 4 illustrates the effect of concurrent adjustments in two input parameters, specifically the solar dish area and the heat pump capacity, on the objective function due to electricity production. Moreover, among the various decision variables, the cooling and heating capacities of the heat pump unit and the area of solar dish stand out as the most influential factors affecting electricity production. Other parameters were found to have a relatively minor effect on the overall electricity production.

Fig. 5 indicates how changing two input parameters simultaneously affects the boiler fuel consumption objective function.

In Fig. 6, the effect of the design variables, especially the area of the solar plate and the cooling and heating capacities of the heat pumps, on the two objective functions, energy production and life cycle cost (LCC), was further investigated.

5. System analysis

Fig. 7 depicts the hourly computation of the ambient temperature in Tehran for the whole year, which spans 8760 hours. Fig. 8 depicts hourly temperature changes in four zones within a given building area. The data demonstrates how the temperature within the building varies when the outside temperature fluctuates. During the summer, the maximum inside temperatures for building units are recorded in June and July.

Fig. 9 indicates the output temperature of solar dish hourly throughout the year in response to changes in Tehran's weather conditions. In Fig. 10, the ambient temperature of Tehran for the whole year, including the covering orator, condenser, and boiler, is presented hourly throughout the year. The data indicates that:

Fig. 11 indicates the demand for hourly hot water during the year, and the proposed system can effectively meet this demand. Fig. 12 shows the system's hourly cooling and heating production yearly. Fig. 13 provides an essential insight into the electricity consumption patterns of buildings in Tehran over a year.

Fig. 14 obtains a primary picture of electricity production throughout the year by renewable system under consideration. In Fig. 15, an hourly analysis compares the electricity generation and consumption rates in residential units over a year.

Fig. 16 shows the annual changes in the thermal comfort coefficient of residential units. These hourly calculations indicate the predicted mean vote (PMV) changes over a year. It is important to note that a positive PMV value corresponds to a warmer feeling for the subject, while a negative PMV indicates a colder perception. The changes of PMV throughout the year are in the range of -0.8 to 1.5. Fig. 17 shows the hourly changes in freshwater production obtained by the reverse osmosis unit over a year. The organic Rankine cycle unit supplies the electricity required for reverse osmosis desalination.

5.1. Environmental and economic implications

The optimized solar-powered cogeneration system demonstrated significant environmental benefits compared with conventional energy supply configurations. Based on the simulation results, annual boiler fuel consumption is reduced to 6,918.0 m^3/year, corresponding to a reduction of approximately 13.1 tonnes CO_2/year (assuming 1.89 kg CO_2 per m^3 of natural gas). Additionally, the system offsets 6,437.4 kWh/year of grid electricity consumption, further reducing indirect emissions from fossil-fuel-based power plants. From an economic perspective, the optimized configuration achieves a life cycle cost (LCC) of $134,130, which is 18.4% lower than that of an equivalent conventional system combining photovoltaic panels with grid electricity and gas-fired boilers for heating. The cost savings arise primarily from reduced fuel consumption and optimized component sizing through RSM. The freshwater produced by the integrated reverse osmosis unit meets WHO drinking water standards, with a total dissolved solids (TDS) level below 500 mg/L. This ensures not only energy self-sufficiency but also high-quality water supply for domestic use. Overall, the proposed system contributes to both climate change mitigation and operational cost reduction, making it an attractive solution for residential complexes in sunny climates [58]. The methodology can be adapted to other cities by recalibrating meteorological inputs and re-optimizing the solar dish area and heat pump capacities according to local energy and water demands

Downloaded from https://iranpaper.ir
https://www.tarjomano.com ترجمه تخصصی این مقاله مورد تایید ایران پیپر

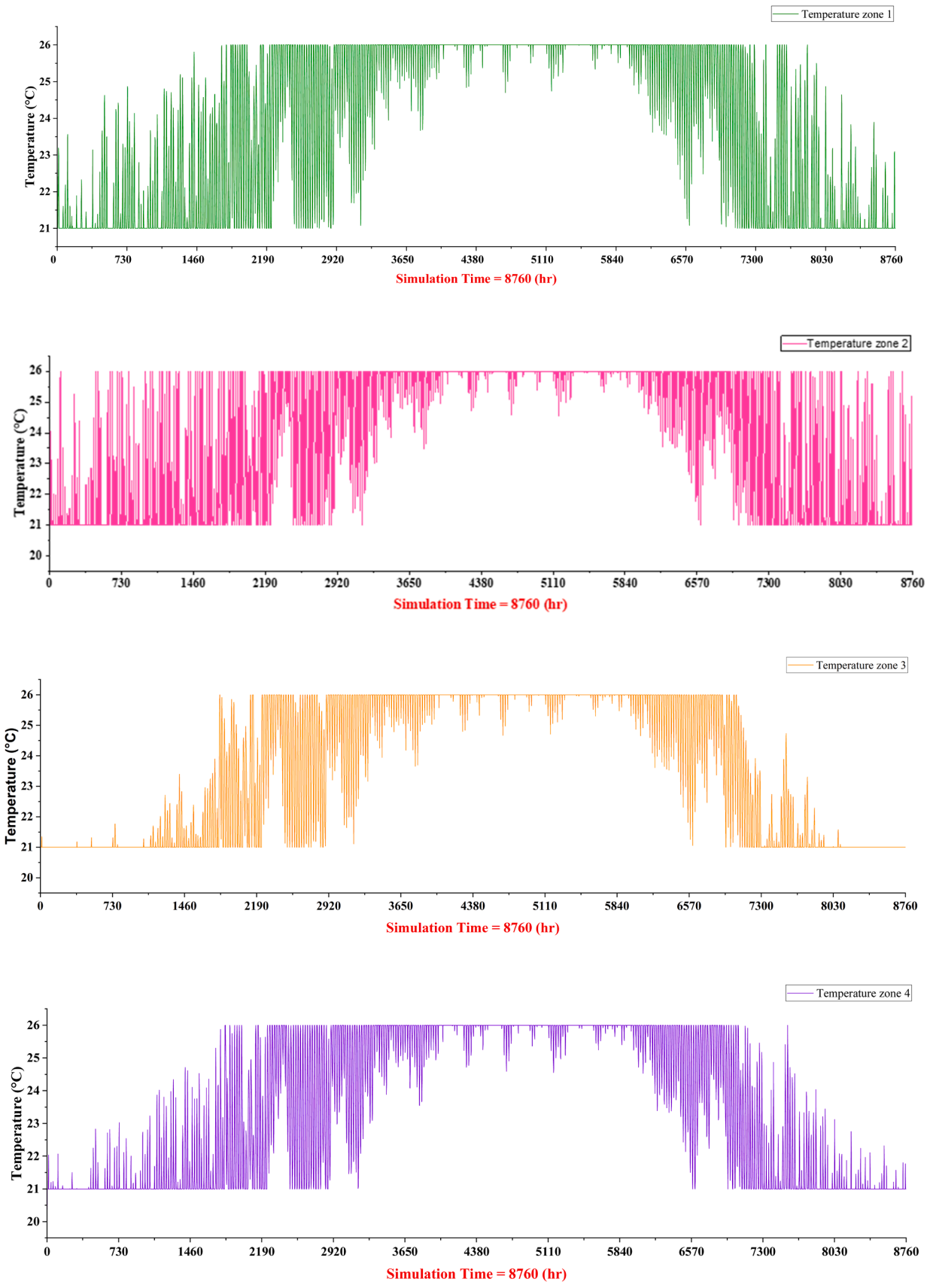

Fig. 8. The temperature of the building throughout the year, hourly.

iranpaper Downloaded from https://iranpaper.ir
https://www.tarjomano.com ترجمه تخصصی این مقاله مورد تایید ایران پیپر

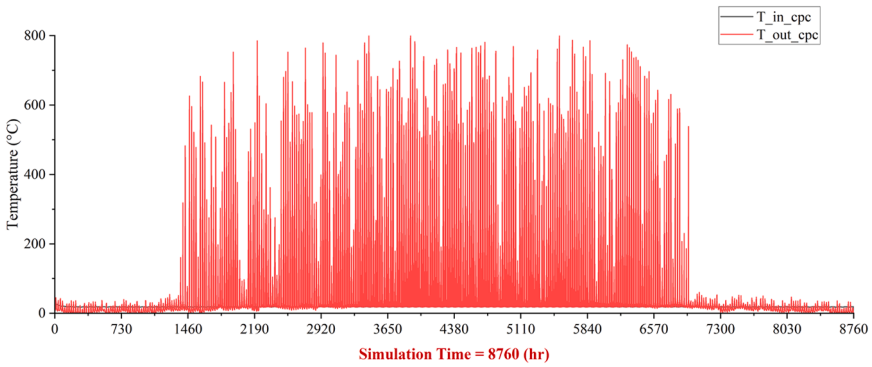

Fig. 9. Output temperature from the solar dish.

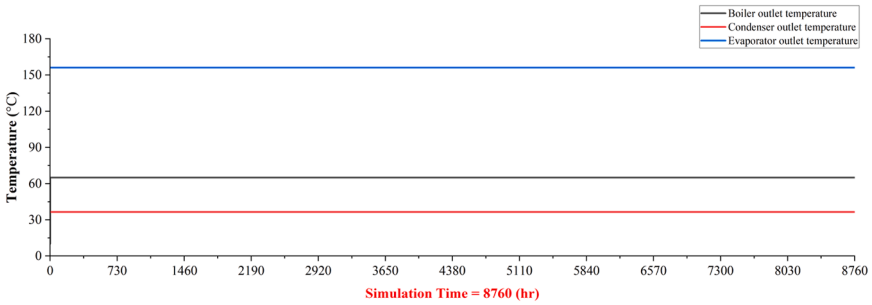

Fig. 10. Output temperature from evaporator, condenser, and boiler.

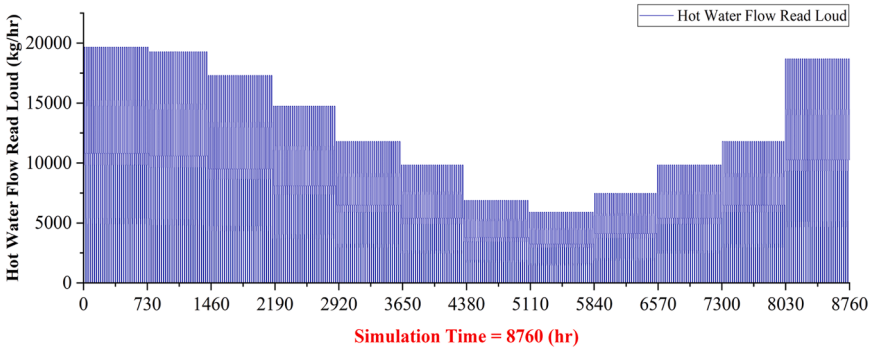

Fig. 11. Required hot water supplies year.

5.2. *Comparative life cycle cost analysis*

To assess the economic competitiveness of the proposed solar-powered cogeneration system, its life cycle cost (LCC) was compared with that of conventional energy supply configurations for a similar residential complex in Tehran. The reference system considered consists of:

- A photovoltaic (PV) array sized to match annual electricity demand,
- Grid electricity supply for shortfalls,
- A natural gas-fired boiler for heating, and
- A standalone reverse osmosis unit for freshwater production.

Based on current market prices for equipment, installation, operation, and maintenance, the 20-year LCC of the reference system is estimated at $164,400. In contrast, the optimized configuration of the proposed system yields an LCC of $134,130, representing a cost reduction of approximately 18.4% over the system lifetime.

The primary contributors to cost savings in the proposed system include:

- Reduced natural gas consumption due to integrated solar thermal input,
- Elimination of separate electricity supply for the RO unit,
- Optimal sizing of the solar dish and heat pump capacities using RSM,
- Shared infrastructure for thermal storage and distribution.

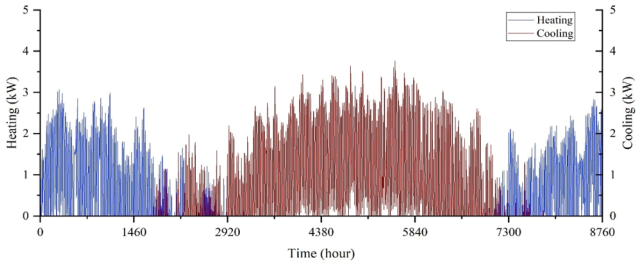

Fig. 12. System production cooling and heating.

Downloaded from https://iranpaper.ir
https://www.tarjomano.com ترجمه تخصصی این مقاله مورد تایید ایران پیپر

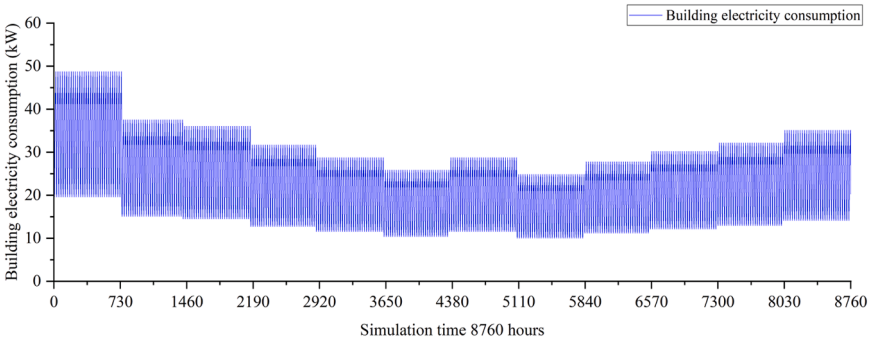

Fig. 13. The amount of electricity consumed by the building.

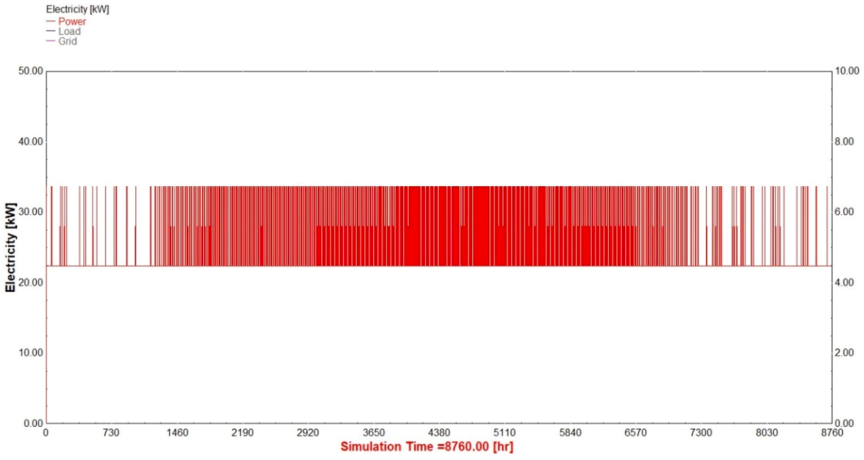

Fig. 14. Annual changes in electricity production rates.

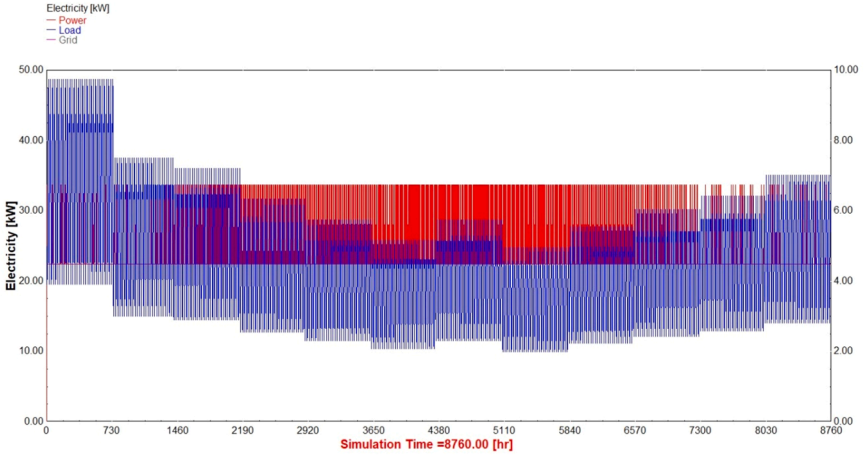

Fig. 15. Hourly comparison of the amount of electricity produced and consumed by the building throughout the year.

Sensitivity analysis further indicates that the economic advantage of the proposed system increases with rising fuel prices and grid electricity tariffs, making it particularly attractive in regions with volatile energy markets. These findings support the viability of the system not only from an environmental standpoint but also in terms of long-term operational cost-effectiveness.

6. Conclusion

The proposed solar-driven cogeneration system was designed to simultaneously meet the annual electricity, heating, cooling, hot water, and freshwater demands of a 100-unit residential complex in Tehran. The system integrates a solar dish receiver, heat pump, organic Rankine cycle (ORC), reverse osmosis desalination unit, thermal storage, and auxiliary boiler. The novelty of the work lies in:

- Combining TRNSYS and EES modeling for transient system simulation of the integrated cogeneration configuration.
- Implementing multi-objective optimization using the Response Surface Methodology (RSM) to balance life cycle cost, boiler fuel consumption, electricity consumption, and thermal comfort.

Downloaded from https://iranpaper.ir
https://www.tarjomano.com ترجمه تخصصی این مقاله مورد تایید ایران پیپر

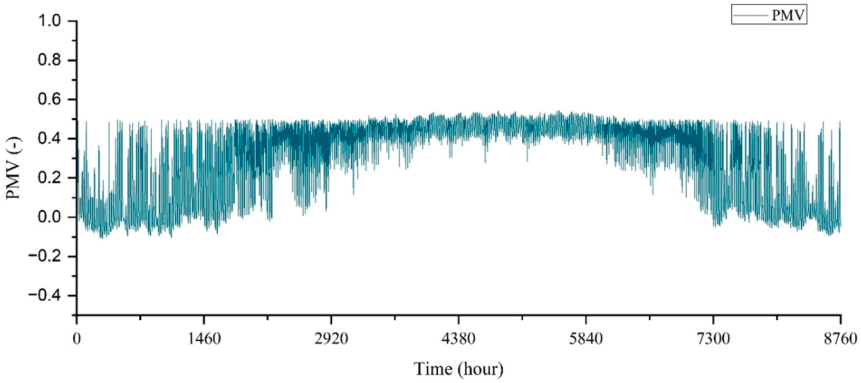

Fig. 16. PMV changes throughout the year.

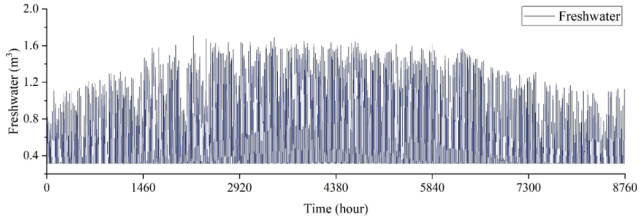

Fig. 17. Changes in freshwater produced by the system throughout the year.

- Providing a comparative evaluation of multiple ORC working fluids, including both conventional and emerging options.
- Assessing environmental benefits and extending applicability to other climates through a scaling law approach.

The optimal configuration identified in this study includes a 101.25 m^2 solar dish area, 20.27 kW cooling capacity, 36.29 kW heating capacity, and benzene as the working fluid. This setup achieves:

- Annual electricity consumption of 6,437.4 kWh/year,
- Boiler fuel consumption of 6,918.0 m^3/year,
- Life cycle cost (LCC) of $134,130,
- Freshwater production with TDS below 500 mg/L, meeting WHO standards.

Compared with conventional PV + grid + boiler systems, the proposed design reduces life cycle cost by approximately 18.4% and cuts CO_2 emissions by over 13 tonnes annually. These benefits, along with the system's multi-output capability, make it a promising solution for sustainable residential energy supply in sun-rich regions. While benzene was identified as the optimal working fluid under the applied multi-objective optimization framework, comparative assessment indicates that R1233zd(E) (non-flammable, ultra-low GWP) and toluene (thermally stable with acceptable efficiency) may be more practical choices for real-world deployment, particularly under strict safety and environmental regulations. This multi-criteria perspective ensures that the study's conclusions are not limited to numerical optimization, but also reflect practical considerations of safety, sustainability, and environmental compliance.

Future work will focus on experimental validation of the integrated system, further evaluation of additional low-GWP working fluids such as hydrofluoroolefins (HFOs) and ionic liquids, and the application of the design methodology to other climatic zones, including Riyadh and Mumbai.

Use of Artificial Intelligence Tools

The authors acknowledge that, as non-native speakers of English, they used ChatGPT (developed by OpenAI) solely to improve the readability, grammar, and linguistic clarity of the article. The use of this AI tool was limited to language editing and did not affect the research design, methodology, data analysis, coding, or interpretation of results. All scientific ideas, conceptual developments, analytical processes, and methodological steps are entirely the original work of the authors. The authors assume full responsibility for the integrity, novelty, and accuracy of the research presented in this article.

CRediT authorship contribution statement

Ali Dezhdar: Investigation, Formal analysis. **Ehsanolah Assareh:** Writing – review & editing, Writing – original draft, Validation, Methodology, Investigation, Conceptualization. **Jagadeesh Kumar Alagarasan:** Writing – review & editing, Validation, Supervision, Resources, Investigation. **Mehdi Hosseinzadeh:** Writing – review & editing, Visualization, Validation. **Saurabh Agarwal:** Writing – review & editing, Validation, Supervision, Formal analysis. **Saleh Mobayen:** Writing – review & editing, Validation, Investigation. **Neha Agarwal:** Writing – review & editing, Software, Resources, Methodology, Investigation, Formal analysis.

Declaration of competing interest

The authors declare that they have no known competing financial interests or personal relationships that could have appeared to influence the work reported in this paper.

References

[1] Pfeiffer B, Mulder P. Explaining the diffusion of renewable energy technology in developing countries. Energy Economics 2013;40:285–96.
[2] Parameshwar, S., et al., Developments in the utilization of heterogeneous catalysts for biodiesel generation: an update on recent advancements. Journal of the Taiwan Institute of Chemical Engineers, 2024: p. 105810.
[3] Broman L, Kandpal TC. PURE-Public understanding of renewable energy. In: World Renewable Energy Congress; 2011.
[4] Zhou Y, et al. Performance study on a new solar aided liquid air energy storage system integrated with organic Rankine cycle and thermoelectric generator. Journal of energy storage 2023;59:106566.
[5] Shahsavar A, et al. A comprehensive review on the application of nanofluids and PCMs in solar thermal collectors: Energy, exergy, economic, and environmental analyses. Journal of the Taiwan Institute of Chemical Engineers 2023;148:104856.
[6] Assareh E, et al. Utilizing Artificial Intelligence (AI) for the optimal design of geothermal cogeneration systems in zero energy building. Results in Engineering 2025:104873.
[7] Hajabdollahi H, et al. Technical and economic evaluation of the combined production cooling, heating, power, freshwater, and hydrogen (CCHPWH) system in the cold climate. Journal of the Taiwan Institute of Chemical Engineers 2022; 133:104262.

Downloaded from https://iranpaper.ir
https://www.tarjomano.com ترجمه تخصصی این مقاله مورد تایید ایران پیپر

[8] Pourmoghadam P, Kasaeian A. Economic and energy evaluation of a solar multi-generation system powered by the parabolic trough collectors. Energy 2023;262:125362.
[9] Zheng N, et al. Techno-economic analysis of a novel solar-driven PEMEC-SOFC-based multi-generation system coupled parabolic trough photovoltaic thermal collector and thermal energy storage. Applied Energy 2023;331:120400.
[10] Wang X, Duan L, Zheng N. Thermodynamic analysis of a novel tri-generation system integrated with a solar energy storage and solid oxide fuel cell–Gas turbine. Applied Thermal Engineering 2023;219:119648.
[11] Prieto J, et al. Integration of a heating and cooling system driven by solar thermal energy and biomass for a greenhouse in Mediterranean climates. Applied Thermal Engineering 2023;221:119928.
[12] Kavian S, et al. Exergy, economic and environmental evaluation of an optimized hybrid photovoltaic-geothermal heat pump system. Applied Energy 2020;276:115469.
[13] Wang X, et al. A dynamic interactive optimization model of CCHP system involving demand-side and supply-side impacts of climate change. Part I: Methodology development. Energy Conversion and Management 2022;252:115112.
[14] Hu Y, Xia X, Wang J. Research on operation strategy of radiant cooling system based on intermittent operation characteristics. Journal of Building Engineering 2022;45:103483.
[15] Saleem MS, et al. Design and optimization of hybrid solar-hydrogen generation system using TRNSYS. International Journal of Hydrogen Energy 2020;45(32):15814–30.
[16] Abu-Hamdeh NH, et al. Numerical investigation of molten salt/SiO2 nano-fluid in the solar power plant cycle and examining different arrangements of shell and tube heat exchangers and plate heat exchangers in these cycles. Journal of the Taiwan Institute of Chemical Engineers 2021;124:1–8.
[17] Assareh E, et al. Techno-economic analysis of combined cooling, heating, and power (CCHP) system integrated with multiple renewable energy sources and energy storage units. Energy and Buildings 2023;278:112618.
[18] Dezhdar A, et al. A transient model for clean electricity generation using Solar energy and ocean thermal energy conversion (OTEC)-case study: Karkheh dam-southwest Iran. Energy Nexus 2023;9:100176.
[19] Takleh HR, et al. Optimization based on the cost, energy, and environmental approaches of a solar-geo system: using real solar data of ParsaAbad-e-Moghan. Journal of the Brazilian Society of Mechanical Sciences and Engineering 2025;47(1):5.
[20] Takleh HR, Zare V, Mohammadkhani F. Exergy/cost-based optimization of a hybrid plant including CAES system, heliostat solar field, and biomass-fired gas turbine cycle. Energy 2025;318:134724.
[21] Farajollahi A, Baharvand M, Takleh HR. Modeling and optimization of hybrid geothermal-solar energy plant using coupled artificial neural network and genetic algorithm. Process Safety and Environmental Protection 2024;186:348–60.
[22] Takleh HR, et al. Proposal and thermoeconomic assessment of an efficient booster-assisted CCHP system based on solar-geothermal energy. Energy 2022;246:123360.
[23] Assareh, E. and A. Dejdar, A transient model for clean electricity generation using solar energy and ocean thermal energy conversion (OTEC)-case study: Karkheh Dam-Southwest Iran. Available at SSRN 4193398, 2022.
[24] Ajour MN, Abu-Hamdeh NH, Mostafa ME. Optimizing and simulating cooling of electric transformer room utilizing genetic algorithm to reduce electricity/water demand by incorporating borehole ground heat exchangers. Journal of the Taiwan Institute of Chemical Engineers 2023;148:104907.
[25] Akrami E, Khalilarya S, Rocco MV. Techno-economic evaluation of a novel bio-energy system integrated with carbon capture and utilization technology in greenhouses. Journal of the Taiwan Institute of Chemical Engineers 2023;148:104729.
[26] Abed AA, et al. Recent advances in parabolic dish solar concentrators: Receiver design, heat loss reduction, and nanofluid optimization for enhanced efficiency and applications. Solar Energy Materials and Solar Cells 2024;273:112930.
[27] Rawa MJ, et al. The impact of using twisted double tube of innovative turbulator on the efficiency of a flat panel solar collector with geometric optimization. Journal of the Taiwan Institute of Chemical Engineers 2023;148:104831.
[28] Zabihian, F. Alternative Approach to Teaching Gas Turbine-based Power Cycles. in 2015 ASEE Annual Conference & Exposition. 2015.
[29] Wang H, et al. A review of the performance and application of molten salt-based phase change materials in sustainable thermal energy storage at medium and high temperatures. Applied Energy 2025;389:125766.
[30] Fernandes, S., et al., This is an open access article under the CC BY license. http://creativecommons.org/licenses/by/4.0/.
[31] Öztop HF, et al. Effects of cooler shape and position on solidification of phase change material in a cavity. Journal of the Taiwan Institute of Chemical Engineers 2024;163:105628.
[32] Rashidi H, Khorshidi J. Exergoeconomic analysis and optimization of a solar based multigeneration system using multiobjective differential evolution algorithm. Journal of Cleaner Production 2018;170:978–90.
[33] Nemati A, Sadeghi M, Yari M. Exergoeconomic analysis and multi-objective optimization of a marine engine waste heat driven RO desalination system integrated with an organic Rankine cycle using zeotropic working fluid. Desalination 2017;422:113–23.
[34] Naseri A, et al. Exergy analysis of a hydrogen and water production process by a solar-driven transcritical CO2 power cycle with Stirling engine. Journal of cleaner production 2017;158:165–81.
[35] Tayeh YA. A comprehensive review of reverse osmosis desalination: Technology, water sources, membrane processes, fouling, and cleaning. Desalination and Water Treatment 2024;320:100882.
[36] Feria-Díaz JJ, et al. Recent desalination technologies by hybridization and integration with reverse osmosis: A review. Water 2021;13(10):1369.
[37] Azman MAN, et al. Development of positively charged polyamide reverse osmosis membrane via polyethyleneimine spray coating for enhanced radionuclide rejection in water treatment. Journal of the Taiwan Institute of Chemical Engineers 2025;172:106135.
[38] Ware, M.J., Establishing an energy efficieny recommendation for commercial boilers. 2000.
[39] Chen N, Chen Y, Zhao H. Heat recovery from cryptocurrency mining by liquid cooling technology. Recent Updates in HVAC Systems. IntechOpen; 2022.
[40] Sun J, Liu Q, Duan Y. Effects of evaporator pinch point temperature difference on thermo-economic performance of geothermal organic Rankine cycle systems. Geothermics 2018;75:249–58.
[41] Jin Y, Gao N, Wang T. Influence of heat exchanger pinch point on the control strategy of Organic Rankine cycle (ORC). Energy 2020;207:118196.
[42] Bett A, Jalilinasrabady S. Optimization of ORC Power Plants for Geothermal Application in Kenya by Combining Exergy and Pinch Point Analysis. Energies 2021;14:6579. 2021, s Note: MDPI stays neutral with regard to jurisdictional claims in published.
[43] Bull J, et al. Low-Temperature ORC Systems: Influence of the Approach Point and Pinch Point Temperature Differences. Energies 2025;18(11):2954.
[44] Fong K, Lee C. Solar desiccant cooling system for hot and humid region–A new perspective and investigation. Solar Energy 2020;195:677–84.
[45] Park S-H, Jang Y-S, Kim E-J. Multi-objective optimization for sizing multi-source renewable energy systems in the community center of a residential apartment complex. Energy Conversion and Management 2021;244:114446.
[46] Dezhdar A, et al. Development of a hybrid renewable energy system for residential complexes in solar-rich regions, harnessing the collaborative power of TRNSYS and the response surface methodology. International Journal of Green Energy 2024;21(16):3740–63.
[47] Afshar S, et al. Dissection of entropy production for the free convection of NEPCMs-filled porous wavy enclosure subject to volumetric heat source/sink. Journal of the Taiwan Institute of Chemical Engineers 2021;128:98–113.
[48] Nafey A, Sharaf M. Combined solar organic Rankine cycle with reverse osmosis desalination process: energy, exergy, and cost evaluations. Renewable Energy 2010;35(11):2571–80.
[49] Nafey A, Sharaf M, García-Rodríguez L. Thermo-economic analysis of a combined solar organic Rankine cycle-reverse osmosis desalination process with different energy recovery configurations. Desalination 2010;261(1-2):138–47.
[50] Xu Y, et al. An improved treble-level assisting optimization strategy to enhance algorithm search ability in heat exchanger network design. Journal of the Taiwan Institute of Chemical Engineers 2021;129:162–70.
[51] Song J, Gu C-w. Analysis of ORC (Organic Rankine Cycle) systems with pure hydrocarbons and mixtures of hydrocarbon and retardant for engine waste heat recovery. Applied Thermal Engineering 2015;89:693–702.
[52] Liang Y, Yu Z. Working fluid selection for a combined system based on coupling of organic Rankine cycle and air source heat pump cycle. Energy Procedia 2019;158:1485–90.
[53] Chiong M, et al. ORC system using R1233zd (E) for waste heat recovery from the upstream process. In: Proceedings of the 7th International Seminar on ORC Power System:(ORC2023). Editorial Universidad de Sevilla; 2024.
[54] Li G. Thermo-economic evaluation of R1233zd (E) as an R245fa alternative in organic Rankine cycle for geothermal applications. Korean Journal of Chemical Engineering 2021;38(11):2195–207.
[55] Chowdhury AS, Ehsan MM. A critical overview of working fluids in organic rankine, supercritical rankine, and supercritical brayton cycles under various heat grade sources. International Journal of Thermofluids 2023;20:100426.
[56] Javed S, Tiwari AK. Performance assessment of different Organic Rankine Cycle (ORC) configurations driven by solar energy. Process Safety and Environmental Protection 2023;171:655–66.
[57] Havens, V. and D. Ragaller, Study of toluene stability for an Organic Rankine Cycle (ORC) space-based power system. 1988.
[58] Shaikh K, et al. Improvement of heat transfer and fouling retardation performance of heat exchanger using green functionalized graphene nanoplatelets additives. Journal of the Taiwan Institute of Chemical Engineers 2023;153:105227.